1 Basic Principles

1.1 Why were GTSM strainmeters developed?

The current instruments were designed in the late nineteen sixties for collection of low frequency strain data as a tool for observation of earth deformations in tectonic and mining applications. In the early nineteen eighties it was applied to earthquake studies in California by the National Earthquake Hazard Reduction Program where the measurement systems provide for remote (off mains grid) installations, using satellite data collection.. The early systems used a multiplexed channel sampling system with each of the channels sampled in turn and sampled only at very low frequencies (30 minute samples). These transducers were always capable of providing high frequency data (to about 100 Hz), and high frequency versions of the system have been available since 1985. The systems deployed in the PBO program measure all channels simultaneously and thus utilize the full available bandwidth of the system. The primary data stream is sampled at 20 Hz.

1.2 What is in a GTSM Strainmeter?

The strain instrument configuration includes five or more independent modules. A minimum of three of these measure strain (change of diameter with time divided by the diameter) on diameters at different orientations in a plane perpendicular to the axis of the instrument. A further component measures the orientation of the instrument in the hole. An additional component is usually included for strain redundancy. At some NEHRP sites a further two components measure tilt from the vertical axis of the instrument. The instruments proposed for the PBO are sized to allow installation in a 6 inch borehole and no tilt meters are currently included, though they can be added as addon modules to future systems.

Construction is totally modular, with each component approximately 170 mm in length. The modules are strain isolated by rigid bulkheads, and dimensioned such that within each module the strain field is transmitted to the transducer system without perturbation. The outer diameter for all modules is a nominal 100 mm and it is cemented into 150 mm diameter holes at a target depth of approximately 200 m. An expansive grout is used to provide preload of the instrument.

1.3 What does it look like?

A cartoon of the instrument is attached. Strain is monitored using the radial component of deformation of the instrument diameter The three strain cells are configured at 120 degrees from each other. At the level of precision and long term stability required, monitoring of the system ageing and performance was routine for earlier NEHRP deployments and additional components (not attached to the outside walls were used to measure these effects.

The sensing transducers are three element capacitances, with a fixed gap reference as featured in figure 1. In the configurations used the position of the moving plate can be monitored to a few picometers. (1 picometer is 1 million millionths of a meter). The three plate system is used to enhance the stability of the measurement system and its independence to environmental perturbations.

Other modules contain an orientation device, which contains an optically encoded magnetic compass (optionally, a magneto-resistive compass or a simple gyrocompass) to determine the attained instrument orientation when it is placed in the borehole. It is not practical at the depths used to control the orientation of the device during deployment. An armored cable (containing typically 16 twisted shielded pairs of conductors) is used as instrument support during deployment.

A two axis tilt meter is available for inclusion in the instrument capsule. The PBO program is not currently deploying quality tilt meters in the field arrays.

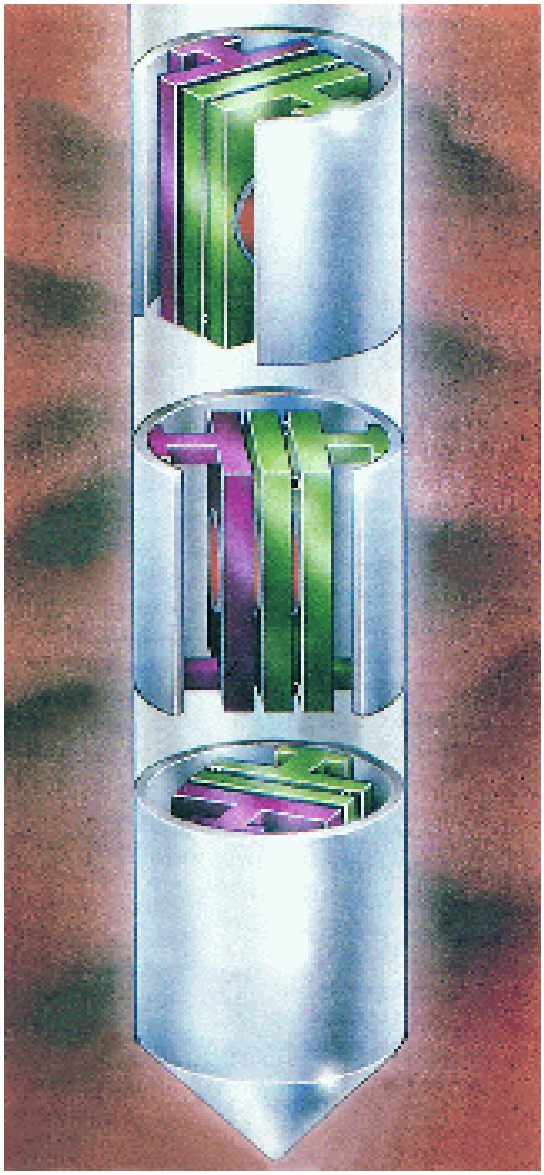

Figure 1. Inside a GTSM Strainmeter

1.4 How is strain measured

Figure 2 shows a schematic drawing of a conceptual layout of a single strain component for this configuration. Two plates of the three plate capacitor are mounted from one side of the instrument cylinder with a fixed and precisely ground inter-electrode gap. The third plate, which in the case shown is the moving plate, is mounted from the opposite diameter. All plates are provided with fringing field guard rings and the reference gap is typically 100 microns. Thermal, mechanical and electrostatic compensations are designed into the geometric configuration of the gauge surfaces and the support structures. The configuration provides mechanical advantage in that the deformation of the cell wall is effectively transferred to the gap measurement area where sensitivity is determined by relative displacement. The configuration shown was the original deployed in California. The raw data is expressed as a ratio of the gap distances. A simple linearization formula is used to provide an output linearly proportional to the change of outer tube diameter. Strain is determined by normalizing this by the gauge diameter.

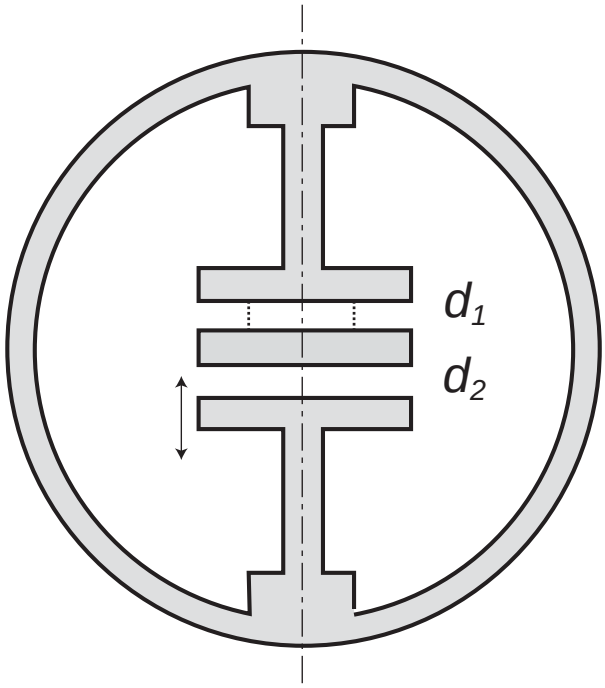

Figure 2: A single strain component

Some current field systems actually use an alternate configuration in which the center plate is mounted from one end of the diameter, and the outer plates are mounted at fixed total gap to the opposite end of a diameter. This configuration provides totally linear intrinsic response. Performance of the two systems can be made equivalent.

1.5 Why are there three or four components?

There are three types of deformation which occurs in the plane perpendicular to the borehole. The first is the areal strain (which relates directly to volumetric strain measured by some other tectonic instruments). In this type of deformation, the change in dimension occurs equally in all directions (azimuths). In most tectonic environments, there are two other strains which are called shear strains. In both types of shear strains, the deformations are different in different directions. These strains are measured by examining the differences in response observed on the three (or more) sensors. These strains are fully defined elsewhere. To isolate these three types of strain (often referred to as ε_a, γ_1 and γ_2) a minimum of three components must be measured.

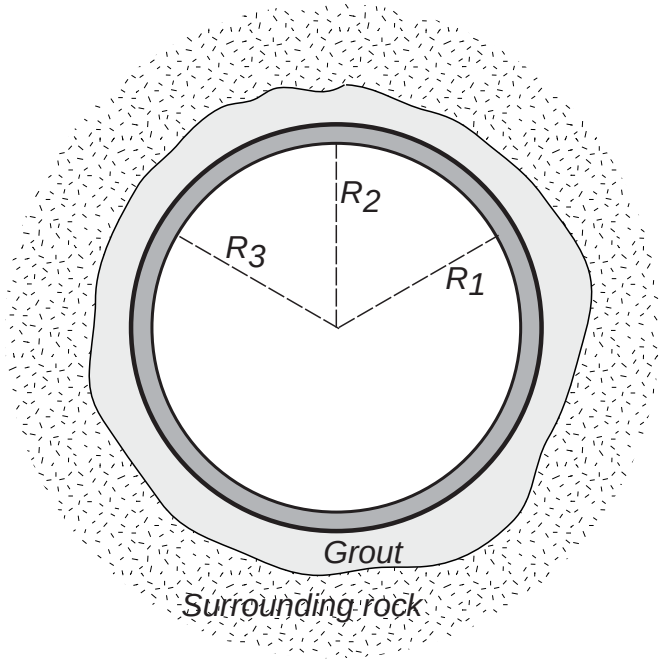

Figure 3: A set of three measurements are performed simultaneously within the instrument, the grout pack and the borehole.

Hence, three components of strain at 120 degrees are monitored continuously on the assumption that along the axis of the instrument package (0.6m) the strain ellipse is constant for changes of strain. This is achieved in practice by carefully locating a zone of uniform rock at least twice the length of the instrument, and filling the hole with expanding grout for some meters both sides of the instrument to produce a near homogenous inclusion as illustrated.

The device is designed to be "moderately hard" so that it is of comparable stiffness as the undisturbed rock mass. It usually has an effective modulus (“stiffness”) not less than 60 to 90 percent of the host environment. The moduli of the instrument is controlled by choice of wall thickness and for most sites is chosen in the range of 1 to 3 gigapascals. Installation of a multi component instrument requires core sampling of representative volumes to determine any anisotropy, to allow good determination of installation target depth, and to provide knowledge of the actual moduli at depth. Though the latter is not essential (see “calibration” later), it can be used to improve the early calibration estimates, and to ensure that the instrument site is not contaminated by any local structural geologic features. Unaco have decided not to provide cores in their normal deployments, and prepare the borehole using tri-cone drilling.

1.6 Does the instrument really see what is happening outside in the rock?

Deformations observed within the instrument are controlled by the instrument effective modulus (which is determined from the wall thickness and materials used), the moduli and thickness of the expansive grout, and the stress concentration around the borehole itself whenever the previous two control parameters are not exactly matched to the rock. A complete analysis allowing for the effects of the series of (welded) concentric rings of materials of different moduli will be provided later.

Principal stress axes (the "directions" of any applied stresses) are preserved through the ring structure except in special cases, but the observed amplitudes can be perturbed significantly. For most applications, an adequate description of the observed strains is obtained by assuming a single deforming ring welded to the rock.

For three cells oriented at 120 degrees from each other, and for the case of plane stress (as distinct from plane strain) here imposed by the lithostatic load along the borehole axis and the near free surface, the three gauges provide observed deformations of U1, U2, U3 which are monitored through time. These measurements allow inversion to the three strain unknowns, i.e. change of hydrostatic strain (ε_a), and change of the two shear components, (γ_1 and $\gamma_{2)}$ with time to be measured. We have shown that the measurements are not contaminated by moderate offsets from location at the center of the borehole, but centralisers are included on the cell stack.

The fidelity of measured strain changes can only be verified with know applied strains and for particular ranges of frequency. There is now considerable published evidence that the instrument implant provides an accurate mapping of the changes of strain applied.

1.7 How is the change in the capacitance measured?

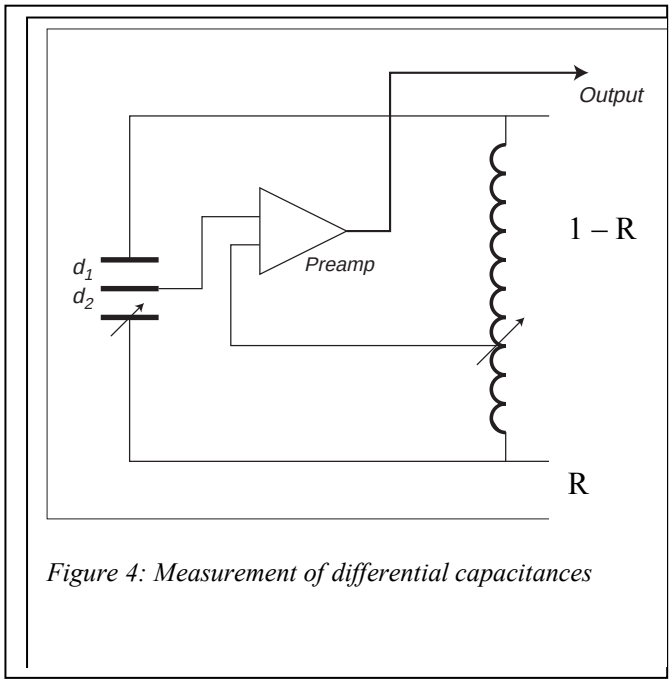

Figure 4: Measurement of differential capacitances

A major consideration in the design of the instrument is its long term stability. The changes of dimension in the rock mass are very, very small. In a typical tectonic environment, the change of the diameter of the borehole will be less than one half of one millionth of one millimeter. To measure such small numbers over time, the measurement system must be made extremely stable.

The stability of the mechanical components can be controlled by choice of materials, fabrication procedures, and specialized thermal destressing of the completed transducer. The electronic stability of the instrument is achieved by the use of ratio transformer bridge technique developed by Thompson (1958), Jones (1967), Gladwin and Wolfe (1975). The system is set up as a differential measurement. Measurement of such differential capacitance changes is achieved to the stability required by use of **passive** voltage division using a device called a ratio transformer.

Figure 4 shows the basic system used. The core elements of the measurement system (three plate deforming capacitor, and ratio Transformer Bridge) are shown. The non retrievable down-hole system is highly simplified with minimal components. For each strain component, the downhole device consists only of a phase stable impedance matching preamplifier with differential line driver, and an isolated protected regulated power supply. In the present instrument a five decade transformer is used, supplemented by three decade digits of out-of-balance analogue to digital conversion. Stability and linearity at the 0.05 percent level is all that is required at the analogue stage of the measurement. Environmental stability of the ratio transformer is better than 2 parts in 10^9 per degree Celsius. The total electronics is stable to 2 parts in 10 ^ 9 over the temperature range 0 to 45 Celsius.

The measurement sensors are placed in a classic bridge configuration. An oscillator simultaneously drives the two capacitances in series and the passive adjustable transformer. When the voltage generated at the variable tap point of the transformer matches the voltage generated by the division ratio of the two capacitances, the bridge system is in balance. Changes in dimension of the capacitances can thus be tracked by changes of the balance point of the ratio transformer. These changes can be tracked to about one part in 100 million over a wide range of conditions still maintaining the passive response of the ratio transformer.

An eight decade composite ratiometric transformer reading, R, (taken as a decimal number between 0 and 1), indicates the proportion of the bridge voltage which appears across the two arms of the bridge, whose down-hole components are the two capacitors, C1 which is fixed and C2, which is deformation dependant. For a moving outer plate configuration, bridge balance occurs when

$(1-R)/R = Z_1/Z_2 = C_2/C_1 = d_1/d_2$ where z is the impedance, C the capacitance, and d the plate separations.

Thus $d_2 = d_1 R/(1 - R)$

Changes in R reflect changes in strain from some arbitrary starting point. Thus, changes of the position of the moving plate are monitored by changes in the ratio R, which is measured to 1 part in 10^8. The fixed distance d1 is usually set at between 0.1-0.2 mm. With an instrument diameter of 100 mm, the mechanical gain permits strain measurement at the gauge at considerably better than 0.1 nanostrain. Effects due to the ground noise will be discussed later. Intrinsic sensitivity of the instrument itself is not a limitation to measurement.

1.8 What electronics are used to measure the changes?

The AC bridge out of balance signals are presented to a switched gain AC amplifier. In mining applications and the early NEHRP stations, the different channels are multiplexed in time for simplicity. The output is synchronously detected with respect to the bridge reference oscillator signal for either real or imaginary components, filtered and presented to an ADC. The ADC measures residual out of balance which is corrected for instantaneous gain and DC offsets as required, and the result is synthesised with the ratio transformer setting to produce an eight digit reading for storage and transmission to a remote data base. At regular intervals a series of self diagnostics are measured to monitor any variations of temperature, reference frequencies, power supply voltages, etc. These diagnostics, together with the dynamic gain coefficients and offset drift estimates are included in the final data stream which is stored on site in Flash RAM. The site may be interrogated for compressed data files at any time for retrieval to the data archive centre.

Stability and performance of the electronics have been verified by measurements against standard ratio transformers under laboratory conditions. Channels operate autonomously and response is flat DC to 20 Hz. A multi-channel digital logging system gathers the data for GPS time tagging, recording, transmission, state of health information and event identification.

1.9 Why use a split bridge measurement system?

The total measurement could be performed downhole with a digital signal the only return. However, this increases the complexity of the downhole system and its probability of failure. The system in use simplifies the downhole system as far as is possible, at the expense of additional complexity at the surface necessary to ensure proper handling of stray capacitance and the requirement of high long term stability.

There are several advantages in use of the bridge measurement system. The first is that the system is not sensitive to variations of the frequency of the bridge oscillator because the synchronous detector (multiplication circuit) tracks any variations which do occur. Long term variations of amplitude are eliminated by regular electronic calibration of any residual out of balance signal amplitude using fixed and highly stable offsets generated on demand from the ratio transformer. Up-hole incremental steps programmed into the ratio transformer measurement protocol provide offsets at the down-hole preamplifier which are exactly equivalent to physical offsets in the transducer system. These offsets are transmitted to the surface; propagate through all amplifiers, DC and AC gain stages and digitizers to provide real time calibration of the system.

The bridge system provides very wide dynamic range for the measurement system. The measurement system is always kept at null balance point, so effects of stray capacitance are minimized, and common mode rejection of spurious sources is kept high.

2 Processing

2.1 What Processing is used to produce strain data?

A general three dimensional strain tensor has six independent components, to completely describe the strain state of a body. At the surface of the earth, the vertical stress is zero, and so the equations for the plane stress case can be used to describe strains in the horizontal plane. In this case, at point P in the body, let the Cartesian components of horizontal displacement be u in the *x* (east) direction, and v in the *y* (north) direction, and the normal convention of compression negative. The strain tensor reduces to three independent components, ε_{xx} ε_{yy} and ε_{xy}, for which

$$\varepsilon_{xx} = \frac{\partial u}{\partial x}; \quad \varepsilon_{yy} = \frac{\partial v}{\partial y}; \quad \varepsilon_{xy} = \varepsilon_{yx} = \tfrac{1}{2}\left(\frac{\partial u}{\partial x} + \frac{\partial v}{\partial y}\right)$$

This definition of strain leads to a formulation for the elongation (i.e. the change in length per unit length), *e*, in a solid body at an angle θ anticlockwise from the x axis for small strains:

$$e(\theta) = \varepsilon_{xx}\cos^2\theta + \varepsilon_{yy}\sin^2\theta + 2\varepsilon_{xy}\cos\theta\sin\theta$$

Or $$e(\theta) = \tfrac{1}{2}(\varepsilon_{xx} + \varepsilon_{yy}) + \tfrac{1}{2}(\varepsilon_{xx} - \varepsilon_{yy})\cos 2\theta + \varepsilon_{xy}\sin 2\theta$$

Thus, elongation at an angle θ is a linear combination of the three independent strain tensor components, ε_{xx}, ε_{yy} and ε_{xy}. In principle three independent observations in the horizontal plane of elongation in a body should be sufficient to determine the strain tensor at that position. This is the primary motivation for the construction of a borehole strain measurement instrument with three independent measurement modules.

While knowledge of the strain tensor components is sufficient to completely characterise the strain field in a plane in a body, it is not necessarily the most useful measure of the deformation of the body. If the strain tensor is known for a body, then the shear strain γ across a vertical plane at an angle θ counter-clockwise from the *x* axis is given by

$$\gamma(\theta) = (\varepsilon_{yy} - \varepsilon_{xx})\sin 2\theta + 2\varepsilon_{xy}\cos 2\theta$$

Traditional engineering analysis has led to a formalism of quantities ε_a, γ_1 and γ_2 such that

$$e_a = \varepsilon_{xx} + \varepsilon_{yy}$$
$$\gamma_1 = \varepsilon_{xx} - \varepsilon_{yy}$$
$$\gamma_2 = 2\varepsilon_{xy}$$

That relation can be expressed as a matrix, such that,

$$\begin{bmatrix} \varepsilon_a \\ \gamma_1 \\ \gamma_2 \end{bmatrix} = \begin{bmatrix} 1 & 1 & 0 \\ 1 & -1 & 0 \\ 0 & 0 & 2 \end{bmatrix} \begin{bmatrix} e_{xx} \\ e_{yy} \\ e_{xy} \end{bmatrix} \qquad \textbf{(1)}$$

These also completely describe the strain state, but isolate the areal or compressional strain ε_a from the shear strain in γ_1 and γ_2. In the investigation of the San Andreas region, this is an advantage in terms of intuitive understanding of the fault processes. γ_1 Is a pure engineering shear which is

maximum across planes oriented northwest or northeast (i.e. at 45 degrees to the coordinate system). γ_2 is a pure engineering shear with maximum shear across planes N-S and E-W. An alternative view of these variables is that γ_1 produces maximum extensional strain in the N-S and E-W directions, whereas γ_2 produces maximum extensional strain in NE-SW and NW-SE directions. In terms of these quantities, the elongation at angle θ is given by

$$e(\theta) = \tfrac{1}{2} e_a + \tfrac{1}{2}\gamma_1 \cos 2\theta + \tfrac{1}{2}\gamma_2 \sin 2\theta \qquad \textbf{(2)}$$

The principal axes of strain in the horizontal plane are defined by directions φ_0 such that shear strain across planes in these directions is zero, and so

$$\tan 2\varphi_o = \frac{\gamma_2}{\gamma_1}$$

For these directions, the extension is

$$e(\varphi_o) = \tfrac{1}{2}(\varepsilon_a + \sqrt{\gamma_1^2 + \gamma_2^2})$$

It is useful to define two further strain parameters, tensor areal or planar hydrostatic strain

$$\mathrm{P} = \tfrac{1}{2}(\varepsilon_{xx} + \varepsilon_{yy}) = \tfrac{1}{2}\varepsilon_a$$

and maximum tensor shear strain (>0 by convention)

$$\mathrm{S} = \tfrac{1}{2}\sqrt{\gamma_1^2 + \gamma_2^2}$$

so that strain in the principal axis directions is given by

$$\varepsilon(\varphi_o) = \mathrm{P} \pm \mathrm{S}$$

The principal strains are thus

$\varepsilon_1 = \mathrm{P} + \mathrm{S}$ (axis of maximum extension)

$\varepsilon_1 = \mathrm{P} - \mathrm{S}$ (axis of maximum compression)

For three horizontal directions at 60 degrees to each other, the elongations to be measured can be represented in a matrix form as follows (using equation (1) above), and are dependent on the geometric orientation matrix relative to the chosen axes:

$$\begin{bmatrix} e_1 \\ e_2 \\ e_3 \end{bmatrix} = \begin{bmatrix} \tfrac{1}{2} & \tfrac{1}{2}\cos 2\theta_1 & \tfrac{1}{2}\sin 2\theta_1 \\ \tfrac{1}{2} & \tfrac{1}{2}\cos 2\theta_2 & \tfrac{1}{2}\sin 2\theta_2 \\ \tfrac{1}{2} & \tfrac{1}{2}\cos 2\theta_3 & \tfrac{1}{2}\sin 2\theta_3 \end{bmatrix} \begin{bmatrix} \varepsilon_a \\ \gamma_1 \\ \gamma_2 \end{bmatrix} \qquad \textbf{(3)}$$

This indicates that deformations of the instrument at particular orientations are **linear** combinations of the tensor components. Areal strains compress the cylinder symmetrically, and shears deform it into an elliptical profile. The tensor components are estimated in principle directly from the measured components by inverting the above matrix. The deformations of the cylinder are the observed data.

Separation into areal and shear strains allows a further simplification of the bore-hole response. It can be shown that instrumental deformation is related to surrounding rock deformation via **separable** areal and shear strain coupling factors, *c* and *d*, and quantities t_{ij} which describe the influence of topography and geology in mapping a regional strain field to strains at the instrument site. Hence, u_i, the actual instrument displacements can be represented by

$$\begin{bmatrix} u_1 \\ u_2 \\ u_3 \end{bmatrix} = \begin{bmatrix} ½ & ½\cos 2\theta_1 & ½\sin 2\theta_1 \\ ½ & ½\cos 2\theta_2 & ½\sin 2\theta_2 \\ ½ & ½\cos 2\theta_3 & ½\sin 2\theta_3 \end{bmatrix} \begin{bmatrix} c & 0 & 0 \\ 0 & d & 0 \\ 0 & 0 & d \end{bmatrix} \begin{bmatrix} t_{11} & t_{12} & t_{13} \\ t_{21} & t_{22} & t_{23} \\ t_{31} & t_{32} & t_{33} \end{bmatrix} \begin{bmatrix} \varepsilon_a \\ \gamma_1 \\ \gamma_2 \end{bmatrix}$$

In terms of vectors and matrices this can be written as

$$\tilde{U} = G.H.T.\tilde{s}$$

where **U** is the deformation vector consisting of the three gauge deformations, G is a direction matrix incorporating the instrument element orientations, H is the coupling matrix consisting of the areal and shear strain coupling factors, T is a matrix describing local topographic and geological influences. **s** is the regional strain state at the measurement site, which is the object of the measurement.

The coupling matrix can be determined by calibration using harmonic analysis of earth tidal signals present in the data. The local topography matrix is determined from knowledge of local topography and geology. Equation (5) enables determination of the regional strain state in terms of the instrument deformations, and the experimentally determined matrices described here.

We also use a further refinement called the gauge multiplier g_i which allows for the mechanical differences for each gauge. These are included in a further multiplier matrix, M, such that

$$\begin{bmatrix} u_1 \\ u_2 \\ u_3 \end{bmatrix} = \begin{bmatrix} 1/g_1 & 0 & 0 \\ 0 & 1/g_2 & 0 \\ 0 & 0 & 1/g_3 \end{bmatrix} \begin{bmatrix} ½ & ½\cos 2\theta_1 & ½\sin 2\theta_1 \\ ½ & ½\cos 2\theta_2 & ½\sin 2\theta_2 \\ ½ & ½\cos 2\theta_3 & ½\sin 2\theta_3 \end{bmatrix} \begin{bmatrix} c & 0 & 0 \\ 0 & d & 0 \\ 0 & 0 & d \end{bmatrix} \begin{bmatrix} t_{11} & t_{12} & t_{13} \\ t_{21} & t_{22} & t_{23} \\ t_{31} & t_{32} & t_{33} \end{bmatrix} \begin{bmatrix} \varepsilon_a \\ \gamma_1 \\ \gamma_2 \end{bmatrix}$$

Ie $\tilde{U} = M.G.H.T.\tilde{s}$

Calibration procedures to determine these in real installations will be discussed later.

Reduction of real time data to far field strains can thus be achieved by a single matrix multiply on the incoming data.

2.2 How does the Instrument respond to the applied strain tensor

The observed deformations of the inner wall of an instrument grouted in a hole are determined by the elastic moduli of the surrounding rock, the grout material and the material of which the instrument is made, the diameter of the borehole, the instrument package and the wall thickness of the instrument.

To provide insight into the effects of these nine parameters, three increasingly complex models have been examined, and a brief indicative summary only will be presented. We have presented extensive analytical solutions in *Hart et al*., 1985, where the dependence of shear (*d*) and areal (*c*) strain response factors on installation geometry and grout and rock elastic parameters is analysed. A summary of the three models we developed there is provided in the following text.

The first model provides a description of the deformation of the wall of an empty borehole. The second model, which we call the single ring model, considers the effect of installing an instrument with annular cross-section in intimate contact with the rock. The third model introduces the effects of a grout introduced between the instrument and the rock wall. This "two ring model" is a critical case for downhole strain instrumentation since grouts must be used to provide coupling and pre-load for the instrument implant. In the examples below, 1 refers to instrument, 2 to grout and 3 to rock. These response factors allow for the fact that for a void space in a solid material, the radial response to areal and shear stresses are different, i.e. that any inclusion will have different stiffness for areal and shear

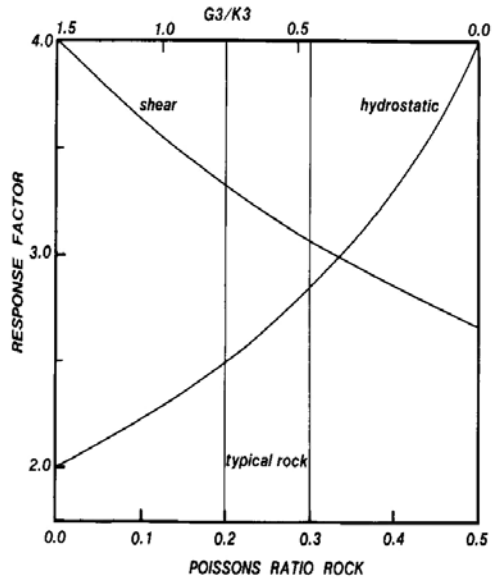

Figure 1 Empty borehole results – dependence on rock Poisson ratio.

fields.

The dependence of response factors (*c* and *d*) on Poisson's ratio of the surrounding rock is shown in the figure above for the empty borehole case. The response factors can be considered to measure the enhanced deformation which would be expected inside an inclusion due to either areal or shear strain in the surrounding rock.

A first order understanding of the design process for an instrument inclusion can be obtained by considering the instrument to be a ring of material in close contact with the bore-hole wall. Figure 2 shows sample results for the case of a one ring model – the dependence of the response factors *c* and *d* on Poisson's ratio, for a range of instrument wall thickness (expressed as a ratio of outer to inner radius). The ratio of the radius of the borehole to the radius of the inner surface of the ring produces a family of curves for particular materials. The hydrostatic response is now significantly lowered for materials of low Poisson's ratio, but the borehole is still soft in shear, so that the shear response factors remain significantly large. We have exploited this in the system design.

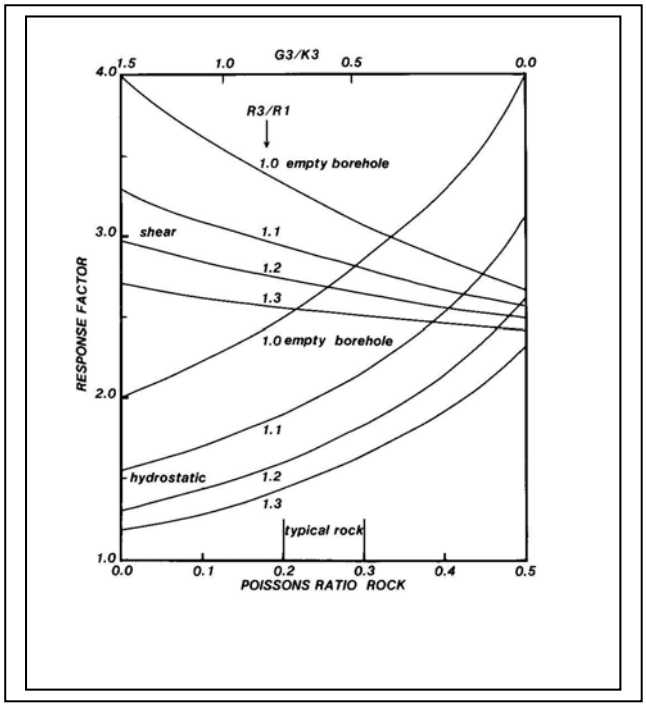

Figure 2 One ring model results for dependence on Poisson ratio, for a range of wall thickness, expressed as ratio of outer to inner radius.

This model could represent the inner surface of an unsupported grout annulus, or the inner surface of an instrument tight coupled to the rock surface. It leads towards a two ring model where the inner ring represents the instrument wall, and the second ring the layer of grout between the instrument and the rock surface. This is a non trivial model, but produces analytical parametric solutions which give a moderately complete and quantitative description of expected internal deformations in strain fields.

The figure below provides some insight into the effects of grout rigidity and thickness using a tow ring model.

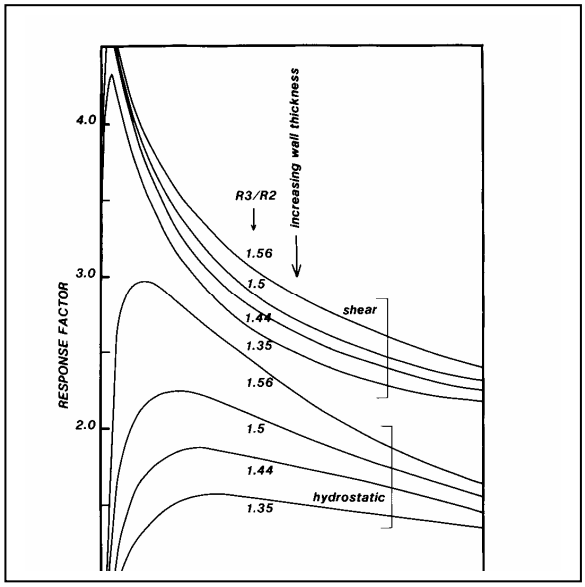

Dependence on borehole radius, for a range of grout rigidity, normalised to instrument rigidity

The two ring model highlights the design trade options in the instrument design over a range of instrument, grout and rock rigidities.

3 Calibration

3.1 What kind of calibrations are available to monitor changes in instrument behaviour?

Because the basic measurement system is an impedance bridge operating at constant temperature at null offset to five decimal places, and because the ratio transformer can be operated as a passive voltage reference source to high precision, it is possible to produce at any time an equivalent displacement offset in the down-hole transducer. This imposed signal is then measured by the system in precisely the same manner as normal displacements using the full complement of cable loading, leakages, AC gain and drift, DC offset gain and drift, power supply and ADC effects. The observed output becomes a precise calibration of system performance at the time, and can be removed from the data stream in a simple linear procedure. This is performed at three hour intervals in the old low frequency systems and at 30 minute intervals in the PBO high frequency version. Quantitative stability of the measurement system is thus known to better than one in 10^8, which is strain of order 10^{-11}. Thus electronic stability and parameterization is easily achieved.

The total borehole inclusion is nowhere near this stable, and calibration of the deformation response of the bore-hole at any particular time is non trivial. The reason for this is that there are many other "signals" in the earth which in a tectonic monitoring exercise easily present as noise. Atmospheric effects are very small on this system, but can still be used for an independent calibration. Ground water effects are particularly problematic for areal strain estimates at some sites because they induce thermo elastic strains of considerable magnitude.

The best one can do to calibrate the total site is to regularly monitor the tidal response of a site (say at twelve month intervals), and to use this to modify the coupling matrix with time. In practice, this is seldom necessary. To this time, there have been no sites which have changed the calibration by more than the uncertainty in its estimate. Even if there had been, one would have to determine whether or not the actual tidal strain amplitude in the earth had changed (for example due to slow changes of hydrology) before assuming a different tidal calibration was needed.

3.2 To what extent does the process of electronic calibration affect the measurement?

The electronic calibration procedure discussed above can be performed without any impact on the measurement data. The crucial issue here is that the dissipation conditions in the down-hole gauge must not be changed by the calibration procedure. This is controlled by the design (coupling, gains etc) of the down-hole electronics.

3.3 What is the frequency response, especially at the high-frequency end?

The low frequency systems in California are flat across their entire operating envelope. The high frequency version to be deployed in PBO is also flat from DC to 20 Hz. This is the result of the fact that bridge frequencies used are in the range of 1 to 3 kHz.

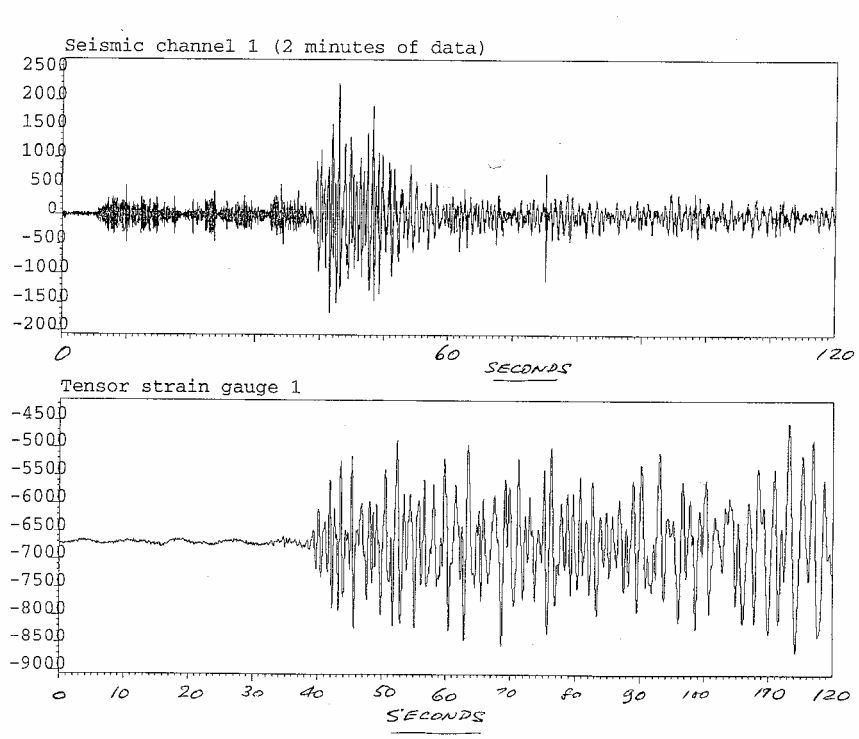

The high frequency response of the GTSM has only been routinely available in the field since the beginning of the PBO program. (The original US program was funded for low frequency only, and proposal to NEHRP to upgrade the sites have not been successful). Some scientists do not see a particular need for high frequency strain measurement since the strain field of a seismic transient can be directly estimated from the seismic response at the site. There is, however, considerable advantage in overlapping the frequency response of the strain meter with the seismic observations in order that any information in the period range say 1 second to 1000 seconds can be seamlessly estimated for compatibly with the seismic estimates.

The seismic response of the GTSM which has been available since the mid eighties has been measured in seismic shot firings at our test site in Australia, and during a Nevada test site explosion in 1986. Sample results are shown in the figure above. A single channel of data from the GTSM instrument sampled at 20 Hz in this case at DLT is plotted, and a single component seismic record near the site is plotted for comparison.

The response is more or less as one would expect, with the strain meter response being particularly rich in late arrival and longer period data. Implementation of routine high frequency strain systems will strongly supplement long period seismometry.

3.4 Are there any trade-offs between sample rate and sensitivity at any frequency?

None are obvious.

3.5 Do sample rate changes alter noise levels in the system in any frequency band?

The front end electronic noise of the measurement system is of order 5 nV per root Hz, and this does not impose limitations comparable with the earth noise over any band of interest.

In the following image, 6 months of data has been used to generate a power spectrum. This image is made up by analysing 10 min data for the longer frequencies, then the 1Hz data for medium frequencies, and finally 20Hz and 100Hz for the high frequency end of the spectrum. Note the rolloff 30Hz is a five pole filter applied prior to the 100 Hz sampling used to provide the 20 Hz primary output.

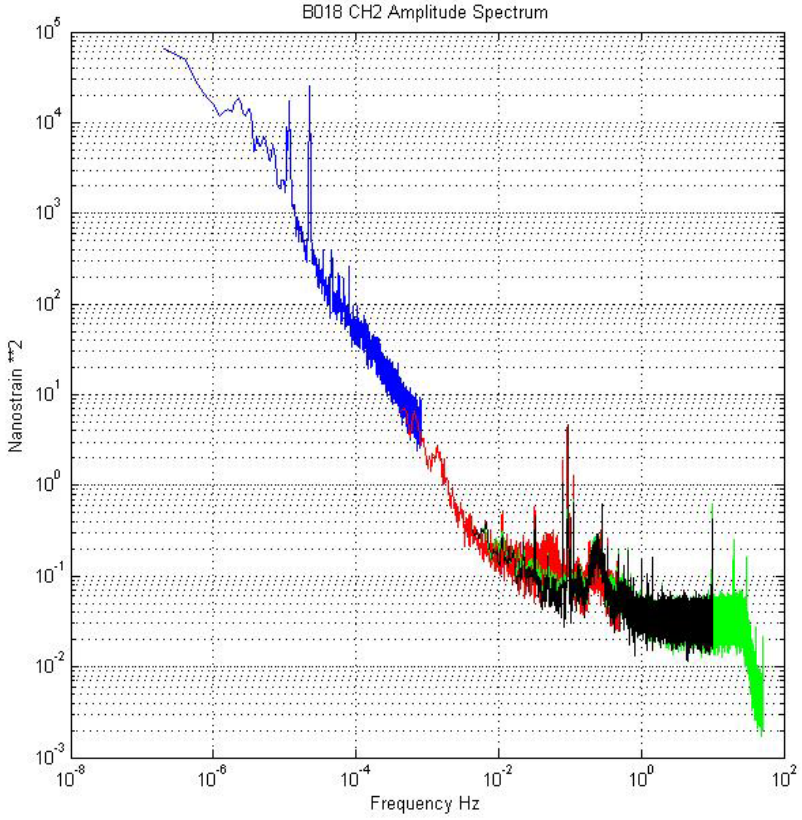

.

At this particular site there is very high level of noise in the period range 100 seconds to 1 second. This microseismic background noise is very site dependent. Spectra of this kind can also be used to provide a reasonable estimate of the lowest anomalous signal detectable within any period range. Following Parseval's theorem, if one needs to examine a particular signal for threshold detection, integration of the spectrum over the period band greater than the period range of interest allows determination of the standard deviation to be expected from assumed-stationary data. A signal excursion with the character of a particular observed anomaly can thus be identified if it exceeds the calculated random walk anomaly for the same time interval. Several alternative approaches to determining the minimum detectable signal have been suggested, e.g. Langbein et al., 1993.

In California, the BTSM data has a noise frequency dependence close to f^2 and for this case it can be shown that the sensitivity A ~=~ $2\pi\sigma$sqrt (τ /T), where σ^2 is the variance of the noise over the interval T. When this function is plotted for daily data, for which the noise level is typically about 3 nanostrain, the result is shown. This indicates a linear anomaly of size 180 nanostrain is only just detectable after 3 months by reason of the ambient noise level which is typical.

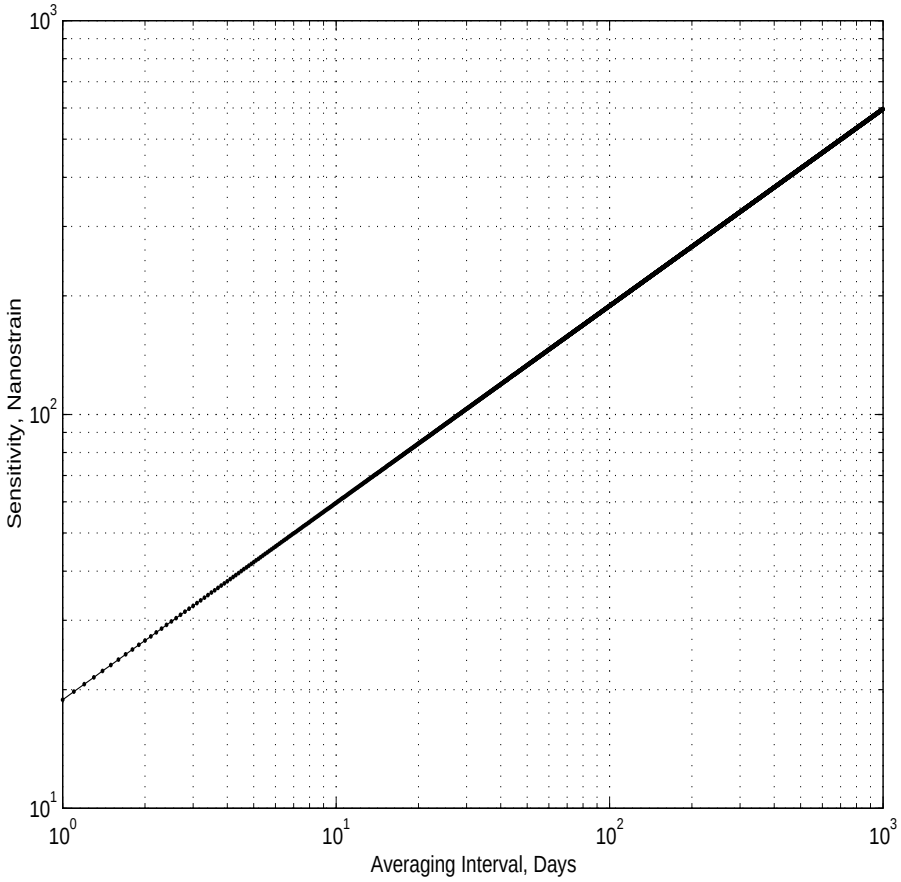

3.6 What are the instrumental limitations on dynamic range?

Arbitrary dynamic range can be provided. Our current choice imposed by the choice of plate gaps and an arbitrary limit of peak deformation of the downhole system is a strain of 10^{-3}. At this level, of static loads (extremely unlikely in tectonics though we have seen them in mining applications), long term creep of the instrument also tends to occur. At the lower end the dynamic range is limited by electronic noise at $10^{-11.}$

The maximum strain which can be accommodated by the measurement system for the PBO systems is 10^{-2}.

3.7 How sensitive is the strainmeter to vertical strain change?

As noted earlier, the vertical strain approaches zero at the surface of the earth. Consequently, variations of the vertical strain in the earth will be strongly attenuated at the shallow depths typically used for these measurements.

The instrument is much stronger in the vertical axis than in the horizontal axes, and the vertical sensitivity of the instrument is predictable using the wall thicknesses and the Poisson's ratio. The design is relatively insensitive to vertical strain. The instrument has the expected low response for atmospheric pressure changes consistent with its matching to the rock mass.

3.8 Advanced Calibration

It should be noted that understanding of the issues discussed in the previous section is **not** required to exploit direct strain measurement.

There are several approaches to in site calibration. Procedures can be based on seismic response, on atmospheric response, on solid earth tidal response, and on relative response of other instruments. As an introduction, calibration by tidal response will be hp[resented here, since most scientists use some method based on the solid earth tidal response.

3.8.1 A priori Calibration

The instrument as produced is calibrated in the laboratory as part of the quality assurance program to verify the fabrication process. This calibration basically verifies the wall thickness response and the interelectrode gap settings. It is more than adequate for most sites for the first several years of operation. This calibration is supplemented by independent calibration of the electronics modules. Calibration is by direct loading of the cells and by hydrostatic compression of the completed units as part of the pressure testing of the cable glands. If correct installation procedures are used, a further highly valuable check calibration is obtained during installation prior to grout setting.

3.8.2 Isotropic Calibration

At most sites, an isotropic calibration (assuming rock isotropy) is initially totally adequate. Even this calibration is difficult to perform within the first 6 to 12 months following installation because the strain rates imposed by the borehole recovery process are large compared with the strain component of the tides. The simplifying assumption (that the half space is isotropic) allows a relatively straight forward procedure to be used. This calibration assumes isotropic behavior of the rock mass in the vicinity of the instrument, but takes account of variations in mechanical properties of each gauge due to slight variations in gap size, etc.

The calibration assumes an areal calibration coefficient ("c"), a shear calibration coefficient ("d"), and gauge multiplying factors ("gi") for each gauge i. These can be combined to result in an areal calibration coefficient ("c_i") and a shear calibration coefficient ("d_i") for each gauge i.

The procedure employs a comparison of theoretical and observed tides, using the two main tidal lines O_1 and M_2. Amplitude and phase are necessary to combine into phasors which can be used during calculations from strain to extension and vice versa. An outline of the basic procedure is as follows:

(a) Calculate theoretical gauge extensions, assuming c=1, d=1 i.e. for the solid rock mass.
(b) Find ratio to observed gauge extensions, to derive g_1,g_2,g_3 multiplying factors
(c) Use these factors to calculate observed strain state ε_a, γ_1 and γ_2
(d) Compare with theoretically determined strain state to derive factors c and d.
(e) Iterate steps (a)... (d) to obtain final c, d, g_1, g_2, g_3

The procedure relies on the general validity of the predicted tidal response of the earth. These tides are in general reasonably well known unless there are nearby water effects. The calibration process **cannot be better than the tidal estimate**, and large errors have been identified in tidal estimates in most studies. Instruments (eg GTSM and UCSD Laser strainmeter) agree with each other much more closely than either do with even a very well documented tidal estimate.

The following steps are typical:

1) Run a tidal package (eg GOTIC) for prediction of tidal amplitudes and phases at site.
Extract from the output, results in the form of a 4x3 matrix, namely:

$e_{11}M_2$ amplitude	$e_{11}M_2$phase	$e_{11}O_1$amplitude	$e_{11}O_1$phase
$e_{22}M_2$ amplitude	$e_{22}M_2$phase	$e_{22}O_1$amplitude	$e_{22}O_1$phase
$e_{12}M_2$ amplitude	$e_{12}M_2$phase	$e_{12}O_1$amplitude	$e_{12}O_1$phase

For this discussion, this will be called the "Theoretical tensor matrix"

Convert this to the "Theoretical Strain State Matrix", viz

$\varepsilon_a M_2$ amplitude	$\varepsilon_a M_2$phase	$\varepsilon_a O_1$amplitude	$\varepsilon_a O_1$phase
$\gamma_1 M_2$ amplitude	$\gamma_1 M_2$phase	$\gamma_1 O_1$amplitude	$\gamma_1 O_1$phase
$\gamma_2 M_2$ amplitude	$\gamma_2 M_2$phase	$\gamma_2 O_1$amplitude	$\gamma_2 O_1$phase

2) Convert the theoretical strain state matrix to a matrix of theoretical gauge extensions th_e_1, th_e_2, th_e_3 at our three gauge angles θ_1 θ_2 θ_3 , assuming initially that c=1, d=1

th_$e_1 M_2$ amplitude	th_$e_1 M_2$phase	th_$e_1 O_1$amplitude	th_$e_1 O_1$phase
th_$e_2 M_2$ amplitude	th_$e_2 M_2$phase	th_$e_2 O_1$amplitude	th_$e_2 O_1$phase
th_$e_3 M_2$ amplitude	th_$e_3 M_2$phase	th_$e_3 O_1$amplitude	th_$e_3 O_1$phase

This can be designated the "Theoretical extension Matrix"

3) Using a tidal analysis program, eg BAYTAP (or equivalent modeling code) on each individual gauge data set, extract the observed results of amplitude and phase for M2 and O1, namely:

obs_$e_1 M_2$ amplitude	obs_$e_1 M_2$phase	obs_$e_1 O_1$amplitude	obs_$e_1 O_1$phase
obs_$e_2 M_2$ amplitude	obs_$e_2 M_2$phase	obs_$e_2 O_1$amplitude	obs_$e_2 O_1$phase
obs_$e_3 M_2$ amplitude	obs_$e_3 M_2$phase	obs_$e_3 O_1$amplitude	obs_$e_3 O_1$phase

4) This is our "Observed Extension Matrix"

Compare amplitudes for each gauge and average results for M2 and O1, to obtain gauge multiplying factors
g_1, g2 and g_3

thus identifying the "Gauge multiplier Matrix"

5) Multiplying the Gauge multiplier Matrix by the Observed Extension_Matrix, and converting from measured extensions to the strain state, form

obs_$\varepsilon_a M_2$ amplitude	obs_$\varepsilon_a M_2$phase	obs_$\varepsilon_a O_1$amplitude	obs_$\varepsilon_a O_1$phase
obs_$\gamma_1 M_2$ amplitude	obs_$\gamma_1 M_2$phase	obs_$\gamma_1 O_1$amplitude	obs_$\gamma_1 O_1$phase
obs_$\gamma_2 M_2$ amplitude	obs_$\gamma_2 M_2$phase	obs_$\gamma_2 O_1$amplitude	obs_$\gamma_2 O_1$phase

This is the "Observed strain state matrix"

6) Compare amplitudes in Observed strain state matrix with Theoretical strain state matrix, average over M_2 and O_1, and obtain values for the areal and the shear calibration factors, c and d.

7) Iterate steps (2) .. to (6), using derived values of c, d, g_1, g_2 and g_3 at each step.

The final result is a value c_i (= c/g_i) and d_i (= d/g_i) for each gauge.

The comparison is done in component form and on radial displacements. In this process it is important to maintain the physics of the instrument itself (it is essentially isotropic and variations of g_i are most unlikely), and to ensure that the shear response is reasonably related to the areal response.

3.8.3 Generalisation of calibration principles – Anisotropic Calibration

The procedure above suggests that a more general form of calibration would incorporate inhomogeneities to account for cross-coupling. The 9 elements of the calibration matrix **S** must be determined from the calibration equations, using known remote strains $\mathbf{s}^R$ and the corresponding transducer readings **e**. This reduces to independently solving three equations, each containing three parameters. For example, the first equation is

$$e_a^R = s_{11}\, e_1 + s_{12}\, e_2 + s_{13}\, e_3$$

and the three parameters are s_{1i}. A minimum of three independent measurements of the variables e_a^R, e_1, e_2 and e_3 are required to solve this equation.

Again, the earth strain tide, the best known signal in strainmeter data, is used as the reference signal, and is obtained from theoretical calculations described later. The observed tidal signal is extracted from the strainmeter data records using standard analysis procedures (Agnew, 1979; Ishiguro and Tamura, 1985), which essentially least-square fit for the amplitudes and phases of sinusoids at the accurately known tidal frequencies. As the procedures effectively narrowband filter the data record at the tidal frequencies, errors in the determined tides from other signals in the strain records (measurement noise, tectonic events or thermally or ground water induced strain disturbances) are largely removed. The raw data records are pre-processed to remove trends, offsets and any bad data. Interpolation over gaps is not required as missing data is managed automatically by the analysis procedures.

For calibration, the largest diurnal and semidiurnal lunar tidal components O_1 (25.82hr) and M_2 (12.42hr) are used instead of the complete tidal record, because tidal components with periods near 24 hours and its harmonics may be thermally contaminated by surface stresses due to temperature. In addition, the strain records are slightly contaminated by atmospheric pressure (~1-4$n\varepsilon$/mbar) and most of the power in pressure is at periods of 24 hours and its harmonics. Each tidal component has two parts (represented here by real and imaginary components), so a total of four sets of tidal variables are available. Small corrections are applied for phase lags introduced by filters in the instrumentation.

Using the four sets of variables provided by the tidal analysis, each of the three over-determined equations (like equation 13) are solved for the elements of the calibration matrix, using least squares techniques. For example, the equation to relate the remote areal strain to the tides measured by the transducers is

$$\begin{bmatrix} \mathrm{Re}(e_a^{O_1}) \\ \mathrm{Im}(e_a^{O_1}) \\ \mathrm{Re}(e_a^{M_2}) \\ \mathrm{Im}(e_a^{M_2}) \end{bmatrix} = \begin{bmatrix} \mathrm{Re}(e_1^{O_1}) & \mathrm{Re}(e_2^{O_1}) & \mathrm{Re}(e_3^{O_1}) \\ \mathrm{Im}(e_1^{O_1}) & \mathrm{Im}(e_2^{O_1}) & \mathrm{Im}(e_3^{O_1}) \\ \mathrm{Re}(e_1^{M_2}) & \mathrm{Re}(e_2^{M_2}) & \mathrm{Re}(e_3^{M_2}) \\ \mathrm{Im}(e_1^{M_2}) & \mathrm{Im}(e_2^{M_2}) & \mathrm{Im}(e_3^{M_2}) \end{bmatrix} \begin{bmatrix} s_{11} \\ s_{12} \\ s_{13} \end{bmatrix}.$$

Though more sophisticated inversion techniques, such as robust inversions or treatment of errors in all variables, could be adopted, the simple method used is justified by the quality of the inversion residuals. A comparison of the residual of the remote strains to the variations expected from tidal measurement errors indicates the quality of the fit. If the residual is acceptable, we estimate the errors

in the calibration matrix elements from the standard deviation σ of the residual, using standard least squares techniques and assuming random measurement errors. This gives the variance of parameter a_i as

$$\sigma_{a_i}{}^2 = \sigma^2 (\mathbf{M^{-1}})_{ii}$$

where **M** is the least squares measurement matrix. If the least squares residual is significantly larger than estimated measurement errors, error in the reference remote strains, inadequacy of the coupling model, or contamination of the strain meter data are indicated.

The errors in a tidal component of angular frequency ω_j are estimated from the variances

$$\sigma_{\mathrm{Re}}{}^2 = \sigma_{\mathrm{Im}}{}^2 = \frac{2}{N} P(\omega_j)$$

where $P(\omega_j)$ is the discrete power spectral density of the noise e_r record in the data record (N samples, sampling period t_s). Orientation errors, transducer factor errors, errors due to variations of modulus and coupling along the bore-hole can be isolated.

The purpose of calibration is to determine the relationship between the remote strains $\mathbf{s}^R$, and the strains $\mathbf{s}^I$ measured by the instrument. As the strains observed are typically small, a linear coupling model

$\mathbf{s}^I = \mathbf{K}\ \mathbf{s}^R$ is the most general form, where **K** is a 3×3 matrix, the coupling matrix. The diagonal elements of this matrix represent direct coupling, for example, of remote areal strain into instrument areal strain, whereas the off-diagonal terms represent cross-coupling. For isotropic coupling, the coupling matrix is

$$\mathbf{K}_H = \begin{bmatrix} c & 0 & 0 \\ 0 & d & 0 \\ 0 & 0 & d \end{bmatrix}.$$

I.e. no cross-coupling is involved.

Cross-coupling can be caused in several ways. One source is the pervasive phenomenon of geological heterogeneity. When small-scale geological heterogeneity is present, the perturbed strains $\mathbf{s}^P$ in the immediate vicinity of a strain meter can be related to the remote strains $\mathbf{s}^R$ by a 3×3 perturbation matrix **P,** as

$$\mathbf{s}^P = \mathbf{P}\mathbf{s}^R$$

provided the wavelengths of the remote strain field are much larger than the heterogeneity wavelengths (Berger and Beaumont, 1976). Off-diagonal terms in **P** of order 0.2 are not unexpected (Berger and Beaumont, 1976; Sato and Harrison, 1990). If the strains just external to the borehole are coupled isotropically into the instrument (as represented by the diagonal matrix $\mathbf{K}_H$), the coupling matrix between the remote and instrument strain states becomes

$$\mathbf{K} = \mathbf{K}_H \mathbf{P}\ .$$

Cross-coupling in the perturbation matrix thus transfers into the coupling matrix.

Other situations which convert simple coupling to the cross-coupled form, including borehole irregularities, anisotropy, topographic perturbations and instrument artifacts, are discussed in Appendix 1. While some of the effects are minor, particularly the instrumental artifacts and topography perturbations for sites with gentle terrain, other effects can be 10% or more, comparable to the more significant geological perturbations.

It is difficult to evaluate the validity of this procedure. The anisotropies have to be kept in a reasonable range constrained by seismically determined moduli in the case of non cored holes.

3.8.4 How have priori models been validated by field measurements?

The best available test for the a priori models discussed above was a calibration of the Pinon Flat GTSM. This has been extensively investigated. Two methods were compared, the first using as a reference, the observed tidal strains measured on the adjacent laser strain meter, and the second method using as Reference Ocean loaded theoretical strain tides which had previously been closely examined for the site.

Calibration using as reference laser strainmeter tides

The LSM provides high precision measurement of the earth tides averaged over a 1km locality at Piñon Flat. These reference tides allow the calibration procedure and the principle of cross-coupling to be tested without the added complexity of uncertainty in theoretical tides. Results are as follows:

Isotropic coupling using the method described earlier produced the coupling parameters

$$c = 1.73 \pm 0.01$$
$$d = 2.86 \pm 0.16 \quad .$$

The corresponding calibration matrix is

$$\mathbf{S} = \begin{bmatrix} 0.386 & 0.386 & 0.386 \\ 0.306 & -0.458 & 0.152 \\ 0.352 & 0.089 & -0.441 \end{bmatrix} \pm \begin{bmatrix} 0.002 & 0.002 & 0.002 \\ 0.017 & 0.025 & 0.008 \\ 0.020 & 0.005 & 0.025 \end{bmatrix} .$$

The areal strains show acceptable agreement in amplitude and phase, though differences are well outside the estimated errors. However, for the shears, a value for d some 30% to 45% smaller than 2.86 is required for $O_1\ \gamma_1$ and $M_2\ \gamma_2$, but a value larger by 25% for $M_2\ \gamma_1$. Phase differences are uniformly larger than expected from error estimates.

Incorporation of cross-coupling into the calibration, produces the calibration matrix

$$\mathbf{S} = \begin{bmatrix} 0.327 & 0.338 & 0.472 \\ 0.209 & -0.474 & 0.295 \\ 0.441 & -0.032 & -0.469 \end{bmatrix} \pm \begin{bmatrix} 0.0156 & 0.013 & 0.021 \\ 0.007 & 0.006 & 0.010 \\ 0.008 & 0.007 & 0.012 \end{bmatrix} .$$

Comparison of cross coupled calibration results with laser strain meter and various earth models at Pinon Flat is shown in

Figure 3. The direct comparison for various components between the LSM and GTSM are shown in the dotted boxes which represent the calculated errors. The two instruments agree more closely with each other than either do with the various earth models. The symbol GB represents Gutenberg-Bullen

earth model, the 1066A earth model is represented by (1066), and the Berger and Beaumont (1976) model is shown as BB. The correlation implied by the ends of the phasor arrows of the measured shears from the two instruments is particularly impressive.

The comparison of LSM and BTSM strain tides in shows that this calibration has brought the BTSM essentially into agreement with the LSM, within measurement errors. The standard deviations of the residuals are $0.22n\varepsilon$ for areal strain and $0.12n\varepsilon$ for shear strains, close to the expected standard deviations of $0.07n\varepsilon$ and $0.07n\varepsilon$. Shear phases have been brought into agreement, and shear amplitudes are consistent for γ_1 and γ_2, for both O_1 and M_2. The coupling matrix is, from equation 12,

$$\mathbf{K} = \mathbf{O}^{-1}\mathbf{S}^{-1} = \begin{bmatrix} 1.778 & -0.159 & 0.268 \\ -0.032 & 2.689 & 0.731 \\ 0.146 & -0.600 & 2.456 \end{bmatrix}.$$

Note also that the diagonal elements are more or less as predicted from the instrument design parameters where c=1.6 and d=2.8 was targeted.

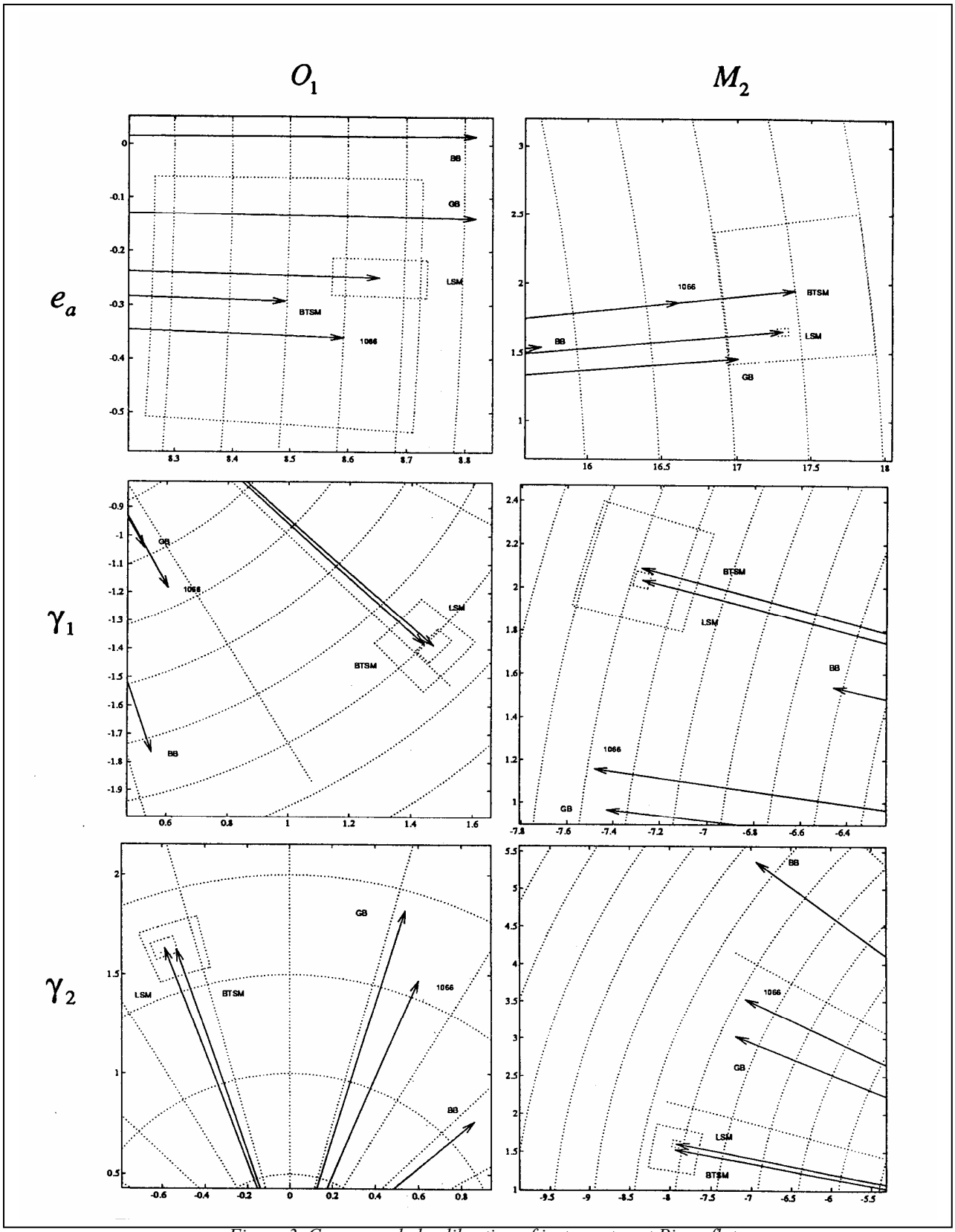

Figure 3 Cross coupled calibration of instrumetns at Pinon flat.

The strain errors from using the calibrations made with theoretical tides, expressed in terms of the error matrix of equation 26, are

$$\begin{bmatrix} \Delta e_a \\ \Delta \gamma_1 \\ \Delta \gamma_2 \end{bmatrix} = \mathbf{E}_{I,T} \begin{bmatrix} {e_a}^R \\ \Delta {\gamma_1}^R \\ \Delta {\gamma_2}^R \end{bmatrix} = \begin{bmatrix} 0.0 & -0.09 & 0.15 \\ -0.01 & -0.09 & 0.25 \\ 0.05 & -0.20 & -0.17 \end{bmatrix} \begin{bmatrix} {e_a}^R \\ \Delta {\gamma_1}^R \\ \Delta {\gamma_2}^R \end{bmatrix}$$

for the isotropic calibration, and

$$\begin{bmatrix} \Delta e_a \\ \Delta \gamma_1 \\ \Delta \gamma_2 \end{bmatrix} = \mathbf{E}_{X,T} \begin{bmatrix} {e_a}^R \\ \Delta {\gamma_1}^R \\ \Delta {\gamma_2}^R \end{bmatrix} = \begin{bmatrix} -0.02 & 0.07 & 0.0 \\ -0.10 & -0.15 & -0.06 \\ 0.19 & 0.17 & 0.18 \end{bmatrix} \begin{bmatrix} {e_a}^R \\ \Delta {\gamma_1}^R \\ \Delta {\gamma_2}^R \end{bmatrix}$$

for the cross-coupled calibration. The isotropic calibration errors are comparable to those for the isotropic calibration with the LSM (equation 27), reflecting the closeness of theoretical and LSM tidal amplitudes. The cross-coupling calibration errors are generally not significantly better, being reduced in some cases but increased in others (for example, coupling of areal strain into γ_2).

These results indicate that a priori models are more than adequate for most intended uses of the tensor strain systems.

This is a slightly surprising result emerging from the complexity of the earth response.

3.8.5 Have calibrations using coseismic earthquake strain offsets been attempted?

Yes.

Incorporation of cross-coupling into the calibration of the Piñon Flat BTSM significantly improved the accuracy of measurements of earthquake strain step signals. The M7.3 Landers earthquake of 1992, some 100km to the north of Piñon Flat, provided a good example. The BTSM strain offsets for this event were well determined, and reasonable dislocation modelling predictions of these offsets can be made using the well constrained source models from geodetic inversions (Hudnut et al., 1994). No other direct strain measurements of the event were available for Piñon Flat (Wyatt et al., 1994; Linde, per comm, 1995), but network averaged strain offsets can be calculated from displacements measured by a nearby 2 colour Electronic Distance Measurement (EDM) network. The table below compares model predictions, EDM strains, and BTSM strains, for the combined Landers earthquake and the Big Bear aftershock three hours later. The EDM strains were obtained by least squares fitting to line-averaged strains, calculated by dividing the displacement offsets in Hudnut's Table 3 by the lengths of the corresponding geodetic lines. Errors are formal fit errors. The BTSM offsets obtained with the cross-coupling calibration (Bx) with the LSM are all within 7% of the model offsets (M), whereas the γ_2 offset for the isotropic calibration (Bi) is in error by 57%. Similar errors are found when the isotropic calibration referenced to theoretical tides is used (Bith). The difference arises from 21% cross-coupling of the large γ_1 offset into γ_2. The EDM γ_2 offset is clearly not compatible with the BTSM offset for the isotropic calibrations, but, within errors, is compatible with the cross-coupled calibration.

The cross-coupling calibration of the BTSM overcomes the criticism that short baseline strain meter measurements are unrepresentative of the strain field in a locality. Representative tectonic strains can now be obtained, provided the reference tides used in the cross-coupled calibration are accurate (here the LSM tides, but ideally more accurate theoretical tides). The accuracy obtained for *both* tidal and tectonic strain measurements from the BTSM indicates that, for periods less than a day, the effective BTSM baseline has been extended to that of the LSM, namely one kilometre. With a cross-coupled calibration, the baseline of borehole strain is determined by the spatial scale of the calibration reference.

We expect cross-coupling to be relevant at the other borehole strainmeter sites, since the geological inhomogeneity at Piñon Flat is not exceptional. Neither are other borehole strainmeter designs, such as the Sacks-Evertson dilatometer, exempt from cross-coupling effects. For the Piñon Flat BTSM, 16% of γ_2 is coupled into areal strain, as shown by equation 27. For an earthquake producing γ_2 three times larger than areal strain at Piñon Flat, neglect of cross-coupling will produce a 50% error in the determined areal strain. In practice, refinement of the accuracy of dilatometer data requires independent estimates of the shear strains.

Though cross-coupling has been identified at Piñon Flat, it was not possible to determine a cross-coupled calibration with theoretical tides, because of demonstrated errors in the ocean load tides and the perturbation estimates. In fact, the accuracy of the cross-coupled calibration was little better than the isotropic calibration. The same difficulties may be expected at other sites. The improvement in accuracy and consequent increased utility of borehole strainmeter sites makes determination of the cross-coupled calibration desirable.

Results are shown for the Landers earthquake in the accompanying Table. Similar comparisons for Big Bear and Joshua Tree earthquakes resulted in a similar assessment: namely that isotropic coupling provides an adequate calibration, but full cross coupled calibration using a locally measured earth tide is preferable if available. These results indicate the quantitative value of strain meter response.

	BTSM (no Xcoupling)	BTSM (with Xcoupling)	BTSM (with Xcoupling & layer correction)	Model (geodetic - Hudnut et al 1994)
e_a	796	757±34	890±34	864
γ_1	-1281	-1188±17	-1246±17	-1171
γ_2	-228	-601±19	-636±19	-718
S (max shear)	1301	1332±18	1399±18	1374
e_a / S	0.612	0.569±0.027	0.636±0.027	0.629
ϕ_{PA} (E of N)	175°	166.6°±0.4°	166.5°±0.4°	164°

Table: Calculated and modelled co-seismic strain offsets from Landers earthquake.

4 Specifications

4.1 What are the diameter, length and weight of the instrument?

Diameter:	100mm nominal
Length overall:	2.2m
Weight (instrument only):	45kg

4.2 How much power is required?

System power is in the order of 20W for a system of four components, including the data logger system.

4.3 How much power is dissipated in the hole?

Approximately 15mA at 5 V continuous.

4.4 What are the major components of a deployed system?

The downhole system is a sealed capsule. An armored cable links the instrument to the surface where a small enclosure is located to house the required uphole electronics and power supplies. Uphole components include:

1. Solar Panel Array
2. Batteries
3. Battery Chargers
4. Power Regulators / Switchers
5. User interface (PC / laptop)
6. Signal Processing - Analogue to Digital Converters.

4.5 What provisions are made for lightening protection and grounding requirements?

All up hole and downhole systems are protected by redundant transorb components. The downhole system is in intimate contact with the earth and this down-hole earth point is the static reference for the whole measurement system. No components of the uphole system are earth at the earth surface or to the casing. This technique (image isolation) ensures that all uphole instrumentation is effectively shielded from local lightening strikes or surges by a few hundred meters of rock. To date, the only down-hole loss has been following a series of two direct hits on an instrument site in close proximity to deep water.

4.6 What type of cable is used?

The support cable for the standard installation is custom designed using standard underwater communications technologies. To ensure adequate lifetime the cable is dual polyethylene bedded.

The cable has been tested for capacitance leakage with time.

Cable dimensions:

Overall cable diameter:	22.5 mm nom ± 0.5 mm
Diameter over armour:	18.7 mm
Diameter under armour:	6.9 mm
Diameter over laying-up:	4.7 mm
Conductor Diameter:	0.9 mm
Earth Diameter:	0.8 mm

Recommended maximum safe pulling/working tension:

Conductors:	0.64 kN
Armour:	5.1 kN

Cable specifications of interest include:

- Conductor Resistance @ 20deg C : 38.4 ohm/km
- Insulation Resistance : 820Mohm.km
- Attenuation at 1 kHz between : 0.118 dB/100m
- Conductor to Screen Characteristic Impedance at 1 kHz : 408 ohm
- Crosstalk between pairs 110db at 1 kHz.

4.7 What type of connector is used to feed the cable to the instrument?

The connector is a customised unit with three independent layers of water block. It is based on conservative stuffing box principles. The inner conductors are reduced to monofilaments buried in a composite epoxy barrier, the inner layer of Decoron is independently sealed in a neoprene pressurised piston block. The armour is then served through 180 degree anchor plates, and the outer water seal is pressure blocked in a second stuffing box. There has not been a field failure of cable head to this time (approximately 140 instrument years for each of four sets of conductors.)

4.8 Do cable dimensions limit the size of other instruments that can be placed in the hole?

Yes. The strain instrument must be the lowest item in the deployment to ensure no azimuthal perturbation of the remote stress field. The cable is laid under tension, and during multiple deployments in a 6 inch borehole, all instrument packages above the system must fit inside a four inch space, and must be encapsulated in tapered instrument capsules.